Journal for Geometry and Graphics
Volume 28 (2024), No. 2, 137–154

Canal Surfaces Containing Four Straight Lines*

Hellmuth Stachel

Vienna University of Technology, Austria
stachel@dmg.tuwien.ac.at

Abstract. A canal surface is the envelope of spheres with centers traversing a spatial curve called spine curve. The spheres contact the envelope along so-called characteristics. These are circles in general. When in limiting poses the spheres become planes, then the characteristics are lines. We focus on cases where the envelope contains lines that contact all spheres and, consequently, are no characteristics. Trivial cases of canal surfaces with infinitely many lines are the right cylinders and cones and the one-sheeted hyperboloids of revolution. If the number of non-characteristic lines on the canal surface is finite, then it is less or equal four. The maximum holds if the four lines are located on a Plücker conoid and intersect each tangent plane of the conoid in concyclic points. We are going to analyse these particular canal surfaces which in general are hard to visualize due to their singularities: They contain cuspidal edges, and the points of the lines are biplanar or uniplanar points of the algebraically closed surface. Symmetric versions are easier to grasp. Even parabolic Dupin ring cyclides and needle cyclides are included as limiting cases when given lines coincide.

Key Words: canal surface, spine curve, Plücker's conoid, pedal curve, concyclic generators

MSC 2020: 51N20 (primary), 53A05, 51N35

1 Introduction

A *canal surface* or *channel surface* $\mathcal{E}$ is the envelope of a smooth one-parameter set of spheres with centers traversing a spatial curve called *spine curve* or *directrix.* In general, the radii of the spheres vary along the spine curve; otherwise we speak of a *tubular surface* or *pipe surface*. The enveloping spheres of the one-parametric set contact the canal surface $\mathcal{E}$ in

*Extended version of the paper "A canal surface containing four straight lines" from the Proceedings of the 9$^{\text{th}}$ International Conference on Engineering Graphics and Design (ICEGD 2024) at the Technical University of Cluj-Napoca/Romania, published in JIDEG (Journal of Industrial Design and Engineering Graphics) **19**/1, 39–44 (2024).

ISSN 1433-8157/ © 2024 by the author(s), licensed under CC BY SA 4.0.

general along circles called *characteristic* (Fig. 1). Consequently, $\mathcal{E}$ is generated by circles with the additional property that the tangent planes along each circle form a cone or cylinder of revolution. The circles together with their orthogonal trajectories form the net of curves of curvature on $\mathcal{E}$.

In limiting cases, an enveloping sphere can become a plane with a straight line as characteristic. On the other hand, the characteristic can shrink to a point, which gives rise to an *umbilic point* of $\mathcal{E}$, or it can be a zero circle without real points.

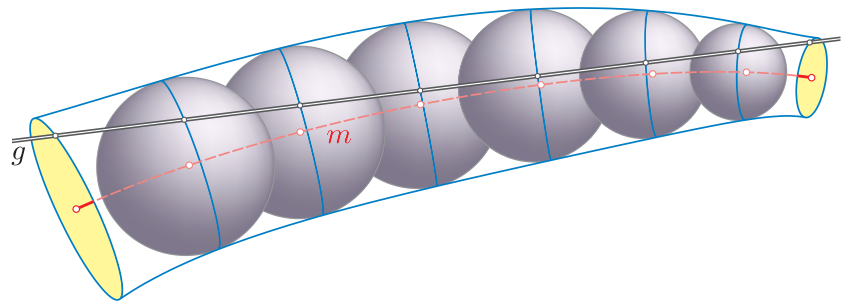

Figure 1: A canal surface as envelope of spheres which contact the line g. The centers of the characteristics form the displayed curve m (red).

Lemma 1. *If all enveloping spheres of a canal surface $\mathcal{E}$ contact a line g, then the points of contact belong to the enveloping surface. Hence, for each point Q of the spine curve of $\mathcal{E}$ the pedal point on g belongs to the characteristic of the sphere centered at Q.*

Proof. Given a canal surface $\mathcal{E}$, let Q_1, Q_2 be two sufficiently close points of the spine curve q. Then the characteristic of the sphere $\mathcal{S}_1$ with center Q_1 is the limit of the intersection with the sphere $\mathcal{S}_2$ with center Q_2 when Q_2 tends along q to Q_1. The circle of intersection $\mathcal{S}_2 \cap \mathcal{S}_1$ lies in the plane of points with equal power with respect to (w.r.t., for short) the two spheres (note [2, p. 49]). This plane is perpendicular to the connection $[Q_1, Q_2]$ of the centers.

Let T_1 and T_2 be the respective pedal points of the common tangent g w.r.t. Q_1 and Q_2. Then, $\mathcal{S}_1$ passes through T_1 and $\mathcal{S}_2$ through T_2. Moreover, the midpoint of the segment T_1T_2 has equal power w.r.t. $\mathcal{S}_1$ and $\mathcal{S}_2$. Therefore, the midpoint is coplanar with the circle of intersection $\mathcal{S}_1 \cap \mathcal{S}_2$. Consequently, at the limit $Q_2 \to Q_1$ and $T_2 \to T_1$ the point T_1 belongs to the characteristic of $\mathcal{S}_1$. The axis of the characteristic is tangent to q at Q_1. □

If all spheres of a canal surface contact two lines g_1, g_2, then the spine curve must be located on the bisector of these lines, which in the case of skew lines is an orthogonal hyperbolic paraboloid $\mathcal{P}_{12}$ and otherwise the orthogonal pair of planes of symmetry (Subsection 2.1). There are trivial cases of canal surfaces which carry infinitely many lines: the right cylinders, the right cones, and the one-sheeted hyperboloids of revolution. In each case, the bisectors of any two lines meet along the axis.

The only nontrivial case of a canal surface where all spheres contact four straight lines[1]is related to a particular ruled surface of degree three, the Plücker conoid. As proved in [8], the four given lines must be concyclic generators of this surface. This means that they intersect

[1]A *parabolic Dupin ring cyclide* (see Fig. 12) contains four lines, but two of them are characteristics, one for each of the two possible generations of the cyclide as a canal surfaces. The other two lines are isogonal trajectories of each family of characteristics, similar to the Villarceau circles of a torus or of non-parabolic Dupin cyclides [5, Fig. 10.18].

each tangent plane τ of the conoid in four points lying on a circle and moreover on the ellipse, which is a component of the intersection between the conoid and the tangent plane τ (Subsection 2.2). The goal of this paper is to analyze and to visualize this particular canal surface, also with regard of its singularities. These singularities are the reason why the shapes of these canal surfaces are hard to grasp and quite different from the standard case as depicted in Fig. 1. All depicted examples reveal that the spine curve is by far no indicator for the shape of $\mathcal{E}$. At the begin we recall the necessary properties of the Plücker conoid.

2 Plücker's Conoid

A *Plücker conoid,* also known under the name *cylindroid,* is a ruled surface of degree three with a finite double line and a director line at infinity (see Fig. 2 or [5, Sect. 11.4]). Using cylinder coordinates (r, ϕ, z), the conoid can be given by the equation

$$\mathcal{C}\colon\ z = c\,\sin 2\phi \tag{1}$$

with a constant $c \in \mathbb{R} \setminus \{0\}$. All generators of $\mathcal{C}$ are parallel to the xy-plane. The z-axis is the double line d of $\mathcal{C}$ and an axis of symmetry. The conoid passes through the x- and y-axis. These two lines c_1, c_2 are axes of symmetry of $\mathcal{C}$ and called *central generators*. The Plücker conoid $\mathcal{C}$ is traced by the x-axis under a motion which is composed from a rotation about the z-axis and a harmonic oscillation with double frequency along the z-axis [12, p. 37]. $\mathcal{C}$ is bounded by the planes $z = \pm c$, which contact $\mathcal{C}$ along the *torsal generators* t_1 and t_2. Their distance $|2c|$ is called the *width* of $\mathcal{C}$.

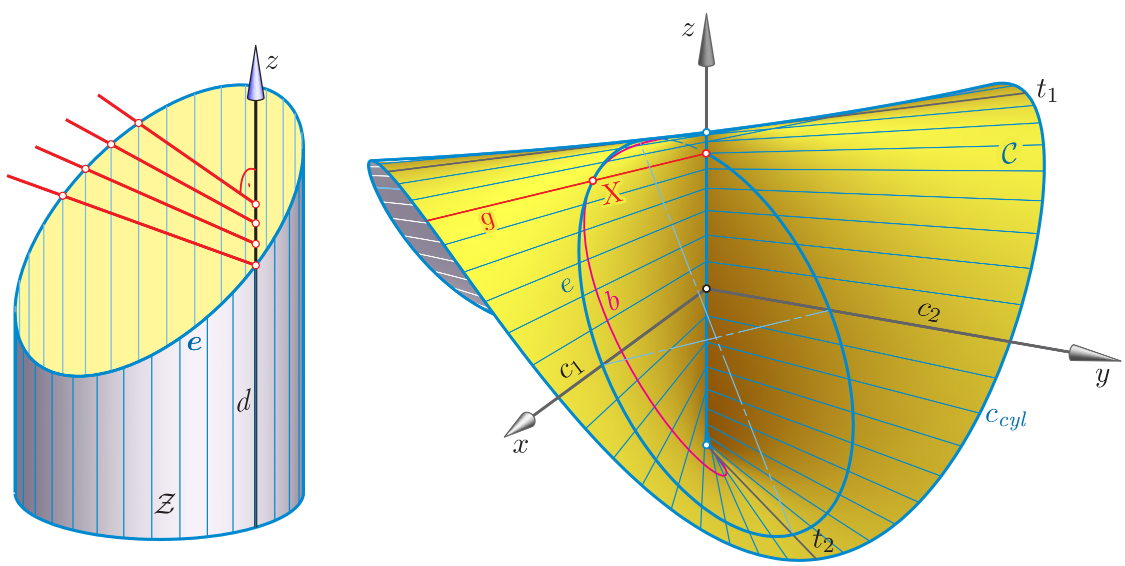

Figure 2: Left: Plücker's conoid $\mathcal{C}$ intersects each right cylinder $\mathcal{Z}$ through the double line d along an ellipse e. The generators of $\mathcal{C}$ meet e and intersect d orthogonally.
Right: Plücker's conoid $\mathcal{C}$ for $c < 0$ along with its central generators c_1, c_2, its torsal generators t_1, t_2, the generator g through X, the ellipse e in the tangent plane τ_X to $\mathcal{C}$ at the point X, and the asymptotic curve $b \subset \mathcal{C}$ which contacts e at X.

The right cylinder $x^2 + y^2 = R^2$ intersects the Plücker conoid $\mathcal{C}$ along a curve c_{cyl} of degree 4 (see Fig. 2),[2] which in the cylinder's development appears as the Sine-curve with amplitude c and wavelength $R\pi$. The generators of $\mathcal{C}$ connect opposite points of c_{cyl}.[3]

The substitution $x = r\cos\phi$ and $y = r\sin\phi$ in (1) yields the Cartesian equation

$$\mathcal{C}\colon\ (x^2 + y^2)z - 2cxy = 0. \tag{2}$$

It shows that reflections in the planes $x \pm y = 0$ map $\mathcal{C}$ onto itself.

For the sake of simplicity, we assume that the xy-plane and all generators of $\mathcal{C}$ are horizontal and the z-axis is vertical. In this sense, the *top view* stands for the image under vertical projection into the xy-plane; a prime will be used to indicate the top views of geometric objects.

Due to the center-angle theorem, the intersection of the Plücker conoid $\mathcal{C}$ with any right cylinder $\mathcal{Z}$ through the double line d gives a curve e which in the cylinder's development shows up as one period of a Sine curve. Therefore, e is an ellipse with principal vertices on the torsal generators. There exists a two-parameter set of ellipses e on the conoid $\mathcal{C}$. Their linear eccentricity equals c, as this is the difference of the respective z-coordinates of a principal vertex and the center of e [4, p. 208]. The secondary vertices of e are located on the central generators c_1 and c_2. Ellipses $e \subset \mathcal{C}$ with the same minor semiaxis are congruent, and their planes have the same slope. Therefore, there is a motion where the ellipse e remains on $\mathcal{C}$ while the points on e run along generators on $\mathcal{C}$. This motion keeps all z-coordinates invariant and appears in the top view as elliptic motion with the circle e' as moving polode (see [4, p. 209]).

Lemma 2. *Let g_1, g_2, g_3 be three non-coplanar lines with an orthogonal transversal d such that no two of the three lines are parallel. Then there exists a unique Plücker conoid $\mathcal{C}$ passing through these lines.*

Proof. We choose a right cylinder $\mathcal{Z}$ which passes through d and does not contact any of the given lines. Then their remaining points of intersection with $\mathcal{Z}$ span a plane that intersects $\mathcal{Z}$ along an ellipse e thus defining $\mathcal{C}$ as shown in Fig. 2, left. □

The remaining intersection between the cubic surface $\mathcal{C}$ and the plane of any ellipse $e \subset \mathcal{C}$ must be a line g passing through the common point of e and d (Fig. 2). This generator g, which is horizontal and therefore parallel to the minor axis of e, shares with e another point X. This must be the point of contact between the conoid and the plane of e. In other words: The tangent plane τ_X to $\mathcal{C}$ at X intersects $\mathcal{C}$ beside the generator g along an ellipse e which appears in the top view as a circle $e' = \mathcal{Z}'$ through d' (Fig. 3).

The top view gives insight into another important property of the ellipse $e \subset \tau_X \cap \mathcal{C}$. For all points P in space with the top view $P' \in e'$ opposite to the top view d' of the double line, the *pedal curve* on $\mathcal{C}$, i.e., the locus of pedal points of P on the generators of $\mathcal{C}$, coincides with e. This holds since the right angles enclosed with generators of $\mathcal{C}$ appear in the top view again as right angles, provided that the spanned plane is not parallel to the double line d. It means conversely that for each point of e the surface normal to $\mathcal{C}$ meets the vertical line through P'. We summarize.

[2] The remaining part of the curve of intersection consists of the lines at infinity of the two complex conjugate planes $x \pm \mathrm{i}y = 0$.

[3] See the models #96 – #100 of the collection of mathematical models at the Institute of Discrete Mathematics and Geometry, Vienna University of Technology, `https://www.geometrie.tuwien.ac.at/modelle/models_show.php?mode=2&n=100&id=0`, retrieved July 2024. All these models originate from Schilling's collection as presented in [7].

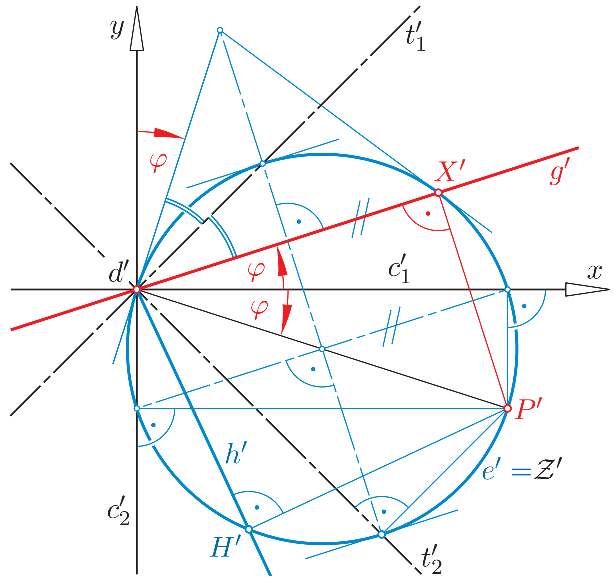

Figure 3: The top view of the Plücker conoid $\mathcal{C}$ shows the pedal point H of the generator $h \subset \mathcal{C}$ w.r.t. all points P with the top view P'. The ellipse e with the circle e' as top view is the pedal curve of $\mathcal{C}$ w.r.t. P. The plane spanned by e contacts $\mathcal{C}$ at the point $X \in g$.

Lemma 3. *All pedal curves of Plücker's conoid $\mathcal{C}$ are planar. For points outside the double line the pedal curves are ellipses with the same excentricity c.*[4]

For points P outside the vertical planes through the torsal generators, the plane spanned by the pedal curve e of P is the tangent plane τ_X at the point X, as shown in Figures 3 and 4. If P lies in the vertical plane through t_1 with $P' \neq d'$, then the plane of the pedal curve e passes through t_2, and the cuspidal point $d \cap t_2$ of t_2 serves as the contact point with $\mathcal{C}$ (note the front view of the pedal curve e_Q of $Q \in q$ in Fig. 10).

2.1 Bisector of two Skew Lines

A classical result states that the *bisector* of two skew lines g_1, g_2, i.e., the set of points X being equidistant to g_1 and g_2, is an orthogonal (or equilateral) hyperbolic paraboloid (Fig. 6). This is reported, e.g., in [6, p. 154] or in [5, p. 64].

Suppose that in an appropriate cartesian coordinate system the two lines g_1, g_2 are given by $z = \pm d$ and $x \sin\alpha = \pm y \cos\alpha$. Then the distance of any space point $X = (x, y, z)$ to g_i satisfies

$$\overline{Xg_i}^2 = x^2 + y^2 + (z \mp d)^2 - (x\cos\alpha \pm y\sin\alpha)^2. \tag{3}$$

Consequently, the bisector of the two lines is defined by the equation $\overline{Xg_1}^2 - \overline{Xg_2}^2 = 0$, i.e.,

$$\mathcal{P}\colon\ 2dz + xy\sin 2\alpha = 0. \tag{4}$$

Conversely, the question for all pairs (g_1, g_2) of lines for which a given orthogonal hyperbolic paraboloid $\mathcal{P}$ is the bisector, was already answered in [7, p. 54] (note also [3]). Their geometric locus is the Plücker conoid

$$\mathcal{C}\colon\ z = c\sin 2\phi \quad \text{for} \quad c := \frac{d}{\sin 2\alpha} \tag{5}$$

[4] Due to P. Appell [1], Plücker's conoid is the only algebraic non-torsal ruled surface with planar pedal curves (note also [4, p. 211]).

with the vertex generators of $\mathcal{P}$ as central generators and the axis of $\mathcal{P}$ as double line. For further details see, e.g., [9].

2.2 Concyclic Generators of Plücker's Conoid

Given a Plücker conoid $\mathcal{C}$, let the ellipse $e \subset \mathcal{C}$ be the pedal curve of any point P. If a sphere $\mathcal{S}$ with the center P contacts some generators of $\mathcal{C}$, then their pedal points w.r.t. P must have equal distances to P. Since they are coplanar with e, they belong to a circle $k \subset \mathcal{S}$ with an axis through P (compare with Fig. 4). The circle k can share at most four points with the ellipse e. Therefore, at most four generators of $\mathcal{C}$ can contact the sphere $\mathcal{S}$ with center P.

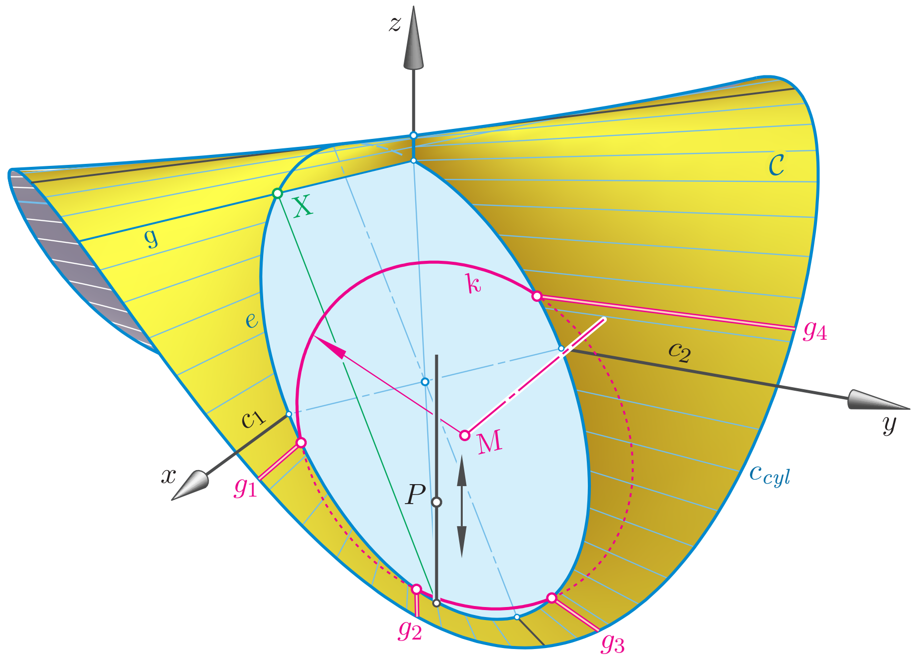

Figure 4: The ellipse e on the Plücker's conoid $\mathcal{C}$ is the pedal curve of the point P and located in the tangent plane τ_X to $\mathcal{C}$ at X. The four concyclic generators $g_1, \dots, g_4$ meet each tangent plane τ_X of $\mathcal{C}$ in points of a circle k. The axis of the circle k is parallel to the vertical plane through P and X.

Definition 1. Four mutually different lines $g_1, \dots, g_4$ in the Euclidean 3-space are called *concyclic* if they belong to a Plücker conoid $\mathcal{C}$ and their points of intersection with a tangent plane to $\mathcal{C}$ are concyclic, i.e., located on a circle.

We recall from [9]:

Lemma 4. *If the generators $g_1, \dots, g_4 \subset \mathcal{C}$ are concyclic, then they intersect each tangent plane τ_X to $\mathcal{C}$ at four concyclic points, provided that in the particular case $g_i \subset \tau_X$ the point of contact X with $\mathcal{C}$ serves as the point of intersection $g_i \cap \tau_X$.*

Proof. Let e_1, e_2 be two ellipses on the Plücker conoid $\mathcal{C}$. Referring to Fig. 5, the top view reveals that lines h' through d' intersect e'_1 and e'_2 at points H'_1, H'_2 which define a similarity $e'_1 \to e'_2$. This induces in space an affine correspondence α_{12} between the ellipses e_1 and e_2 and consequently between their carrier planes. The torsal generators and the central generators

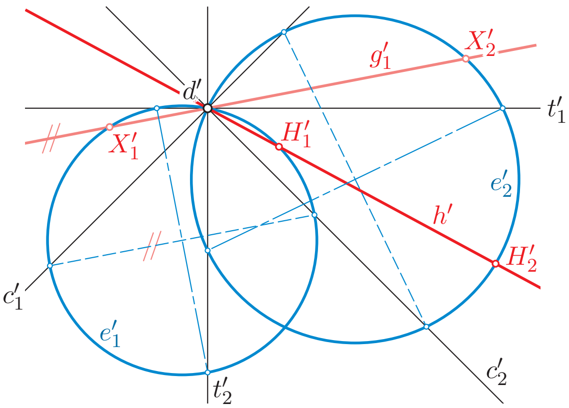

Figure 5: This top view shows that generators h of a Plücker conoid $\mathcal{C}$ intersect different tangent planes at points H_1, H_2 that correspond each other in an affine transformation α_{12}.

of $\mathcal{C}$ indicate that α_{12} sends the vertices of e_1 to vertices of e_2. Using appropriate coordinates (x_1, y_1) and (x_2, y_2) in the respective planes, the correspondence can be expressed in the form

$$\alpha_{12}\colon (x_1, y_1) \mapsto (x_2, y_2) = (\lambda x_1, \mu y_1)$$

with

$$e_1\colon F(X_1) := \frac{x_1^2}{a^2} + \frac{y_1^2}{b^2} = 1 \to e_2\colon \frac{x_2^2}{a^2+k} + \frac{y_2^2}{b^2+k} = 1, \quad \text{i.e.} \quad \lambda^2 = \frac{a^2+k}{a^2},\ \mu^2 = \frac{b^2+k}{b^2}.$$

If (X_1, X_2) and (M_1, M_2) are two pairs of points corresponding under α_{12} with $X_1 = (x_1, y_1)$ and $M_1 = (m_1, n_1)$, then holds

$$\overline{X_2M_1}^{\,2} - \overline{X_1M_2}^{\,2} = k[F(X_1) - F(M_1)],$$

since

$$\lambda^2 - 1 = \frac{k}{a^2} \quad \text{and} \quad \mu^2 - 1 = \frac{k}{b^2}$$

imply

$$\begin{aligned}\overline{X_2M_1}^{\,2} - \overline{X_1M_2}^{\,2} &= (\lambda x_1 - m_1)^2 + (\mu y_1 - n_1)^2 - (\lambda m_1 - x_1)^2 - (\mu n_1 - y_1)^2 \\ &= (\lambda^2-1)x_1^2 + (\mu^2-1)y_1^2 + (1-\lambda^2)m_1^2 + (1-\mu^2)n_1^2 = k[F(X_1) - F(M_1)].\end{aligned}$$

Let M_2 be the center of the circle k_1 through the intersection points $X_1 \in e_1$ of four concyclic generators of $\mathcal{C}$ (note Fig. 4). Then the α_{12}-images $X_2 \in e_2$ have equal distances to M_1, since

$$\overline{X_2M_1}^{\,2} = \overline{X_1M_2}^{\,2} + k[1 - F(M_1)].$$

If e_1 and e_2 are congruent, then follows $k = 0$ and $\overline{X_2M_1} = \overline{X_1M_2}$. In other words, k_1 and k_2 are congruent, too.

An alternative proof in [8, p. 60] is based on Desargues's involution theorem [2, Sect. 7.4] which is applied to the conics pencil spanned by e_1 and k_1. □

Theorem 1. *If four lines $g_1, \dots, g_4$ are concyclic, then there exist infinitely many spheres which contact these lines.*

Remark 1. According to [8, Satz 4], there are only two cases where four mutually skew lines $g_1, \dots, g_4$ have a continuum of contacting spheres: The given lines are either concyclic or they belong to a hyperboloid of revolution[5]. In the first case, the six bisecting hyperbolic paraboloids $\mathcal{P}_{ij}$ of the pairs (g_i, g_j), $i, j \in \{1, \dots, 4\}$, $i \neq j$, belong to a pencil. In the latter case, the paraboloids share the hyperboloid's axis. For similar problems see [10].

Proof. By virtue of Lemma 2, the first three given lines g_1, g_2, g_3 with the common orthogonal transversal d define a Plücker conoid $\mathcal{C}$. The bisecting hyperbolic paraboloids of the pairs (g_1, g_2) and (g_1, g_3) share the vertical axis d and intersect each of the infinitely many horizontal planes along two concentric orthogonal hyperbolas with different asymptotes. These hyperbolas must meet at two real diametrical points which are centers of spheres tangent to the three lines. The pedal points w.r.t. such a center P span a plane which contains the pedal curve e of P on $\mathcal{C}$. On the other hand, the contacting sphere $\mathcal{S}$ with center P intersects the plane of e along the circumcircle k of the three pedal points. The circle k and the ellipse e share a fourth point, and by virtue of Lemma 4 this point belongs to the fourth given generator $g_4 \subset \mathcal{C}$ which contacts the sphere $\mathcal{S}$, as well. □

Corollary 1. *If all spheres of an irreducible algebraic canal surface contact a finite number of lines, then this number is less or equal to four.*

Let three given lines g_1, g_2, g_3 according to Lemma 2 define the Plücker conoid $\mathcal{C}$. Referring to the notation in the proof above, it can happen that the circumcircle k contacts the ellipse e at any point. Then the line g_4 coincides with one of the three given lines. This implies a contact between the conoid $\mathcal{C}$ and the envelope of the infinitely many spheres.

Suppose that two out of four concyclic lines intersect each other on d. Then also the remaining two lines must be intersecting, since in this case the center of the circumcircle k is located on the principal axis of the ellipse $e \subset (\tau_X \cap \mathcal{C})$. We call this an *intersecting case* in contrast to the *skew cases*. Another symmetric position of the concyclic lines arises when the circle k is centered on the secondary axis of e. This position is again independent of the choice of the tangent plane τ_X.

3 The Envelope of the Spheres that Contact four Concyclic Lines

By virtue of Lemma 1, a canal surface whose spheres contact four lines, passes through these four lines. The only non-trivial case is the envelope $\mathcal{E}$ of the spheres as mentioned in Theorem 1.

Theorem 2. *Given four concyclic lines $g_1, \dots, g_4$ on the Plücker conoid $\mathcal{C}$, let $\mathcal{E}$ be the envelope of the contacting spheres.*

If the given lines are mutually skew, then the spine curve of $\mathcal{E}$ is a rational quartic q symmetric w.r.t. the double line d of $\mathcal{C}$ (Fig. 6). The top view of q is an equilateral hyperbola with the top views of the torsal generators of $\mathcal{C}$ as asymptotes (Fig. 8). The envelope $\mathcal{E}$ consists of two components symmetric w.r.t. d.

In the intersecting case, the spine curve of $\mathcal{E}$ splits into two parabolas in the vertical planes through the torsal generators. The parabolas are congruent, they share axis d and vertex and open to different sides.

[5] This was the solution of a problem posed in [3] and related to the isotropy of serial robots.

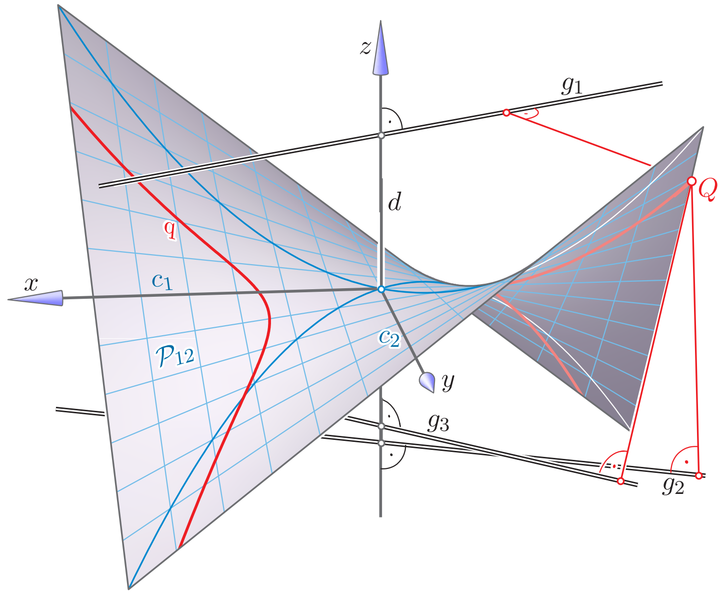

Figure 6: Spine curve q of the canal surface that envelops all spheres which contact the skew lines g_1, g_2 (with bisector $\mathcal{P}_{12}$) and the line g_3.

Proof. Let φ_i for $i \in \{1, \dots, 4\}$ be the polar angle of g_i on the Plücker conoid $\mathcal{C}$. Then, according to (1), g_i has the z-coordinate $z_i := c \sin 2\varphi_i$. By (3) the distance of any space point $X = (x, y, z)$ to g_i satisfies

$$\overline{Xg_i}^2 = x^2 + y^2 + (z - z_i)^2 - (x \cos\varphi_i + y \sin\varphi_i)^2.$$

Hence, the bisecting paraboloid $\mathcal{P}_{ij}$ of the generators $g_i, g_j \subset \mathcal{C}$ obeys the equation $\overline{Xg_i}^2 - \overline{Xg_j}^2 = 0$, i.e., because of $2(\sin^2\varphi_i - \sin^2\varphi_j) = \cos 2\varphi_j - \cos 2\varphi_i$

$$\mathcal{P}_{ij}\colon \frac{1}{2}(\cos 2\varphi_j - \cos 2\varphi_i)(x^2 - y^2) - (z_i - z_j)\left(\frac{xy}{c} + 2z\right) + (z_i^2 - z_j^2) = 0. \tag{6}$$

All paraboloids with $z_i \neq z_j$ intersect the vertical planes $x \pm y = 0$ through the torsal generators t_1, t_2 along congruent parabolas with the parameter c.

In the intersecting case with $z_1 = z_2$ and $z_3 = z_4$ the bisectors $\mathcal{P}_{12}$ and $\mathcal{P}_{34}$ split into the two vertical planes through t_1 and t_2. The other symmetric choice with $\varphi_2 = -\varphi_1$ and $\varphi_4 = -\varphi_3$ results in identical paraboloids $\mathcal{P}_{12} = \mathcal{P}_{34}$ satisfying $xy + 2cz = 0$ in accordance with (5) and (4). This paraboloid intersects the Plücker conoid $\mathcal{C}$ orthogonally along the two central generators (note [5, Fig. 2.39]).

The bisectors $\mathcal{P}_{12}$ and $\mathcal{P}_{13}$ share a spatial curve q of degree four, and each point $P \in q$ is the center of a sphere $\mathcal{S}$ which contacts g_1, g_2 and g_3. As explained before, $\mathcal{S}$ must also contact the line g_4 which completes the concyclic quadruple.[6] We obtain the equation of the top view q' of q as a linear combination of the equations of $\mathcal{P}_{12}$ and $\mathcal{P}_{13}$ after the elimination of z.

(a) In the skew case, the quartic q is irreducible. Its equation has the form

$$q'\colon u(x^2 - y^2) = v \quad \text{with} \quad u, v \in \mathbb{R} \setminus \{0\}, \tag{7}$$

[6] As proved in [8], the four lines $g_1, \dots, g_4$ are concyclic if and only if the (4×5)-matrix with the rows $(1, z_i, z_i^2, \sin 2\varphi_i, \cos 2\varphi_i)$ for $i = 1, \dots, 4$ has a rank ≤ 3.

namely

$$u := z_1(\sin^2\varphi_2 - \sin^2\varphi_3) + z_2(\sin^2\varphi_3 - \sin^2\varphi_1) + z_3(\sin^2\varphi_1 - \sin^2\varphi_2),$$
$$v := (z_2 - z_1)(z_3 - z_2)(z_1 - z_3),$$

hence

$$u = -\frac{1}{2}\det\begin{pmatrix}1 & z_1 & \cos 2\varphi_1\\ 1 & z_2 & \cos 2\varphi_2\\ 1 & z_3 & \cos 2\varphi_3\end{pmatrix}, \quad v = -\det\begin{pmatrix}1 & z_1 & z_1^2\\ 1 & z_2 & z_2^2\\ 1 & z_3 & z_3^2\end{pmatrix}.^7 \qquad (8)$$

Consequently, q' is an equilateral hyperbola with the semiaxis $\sqrt{|v/u|}$ and the asymptotes $x \pm y = 0$, which are the top views of the torsal generators t_1, t_2 of $\mathcal{C}$ (Fig. 8). In order to compute the z-coordinate of the points of q, we use the equation of $\mathcal{P}_{12}$ which is linear in z. Therefore, q is rational. According to the two branches of the hyperbola q' the envelope $\mathcal{E}$ has two components; one arises from the other by a reflection in the double line d.

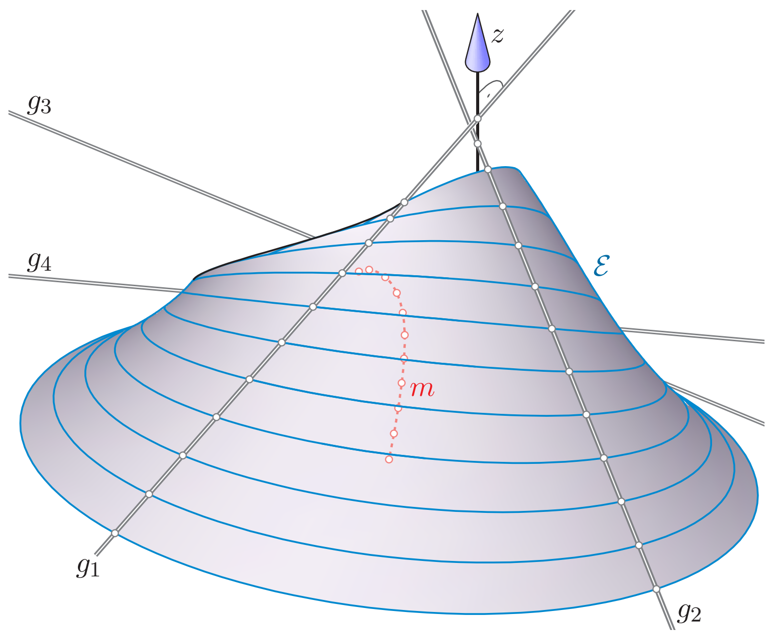

Figure 7: A singularity-free portion of the canal surface $\mathcal{E}$ through the mutually skew concyclic lines $g_1, \dots, g_4$ along with the locus m of the characteristics' centers. The black curve is an edge of regression.

(b) In the intersecting case, we can assume $z_1 = z_2 \neq z_3$. Then $\mathcal{P}_{12}$ splits into the vertical planes through t_1 and t_2. Each of them intersects $\mathcal{P}_{13}$ along a parabola with the vertical axis d and the parameter $|c|$. □

Each point Q of the spine curve q is the center of a sphere $\mathcal{S}$ which has a real contact with the enveloping canal surface $\mathcal{E}$. The characteristic k of $\mathcal{S}$ is the circumcircle of the pedal points of $g_1, \dots, g_4$ w.r.t. Q and located in a tangent plane τ_X of $\mathcal{C}$. The generator g in τ_X is horizontal; the contact point X belongs together with Q to a vertical plane which is parallel to the principal axis of the ellipse $e \subset (\tau_X \cap \mathcal{C})$ (note Fig. 4). This vertical plane contains also the center M of k which is the pedal point of the plane τ_X w.r.t. Q. Therefore, the axis

[7] According to Footnote 6, the column vector $(\cos 2\varphi_i)$ for $i = 1, \dots, 4$ in the (4×5)-matrix can be represented as a linear combination of the column vectors (1), (z_i) and (z_i^2). Due to Cramer's rule, we obtain $v/2u$ as the coefficient of the z_i^2 in this linear combination.

$[Q, M]$ of the characteristic k, which is tangent to the spine curve q at Q, has a top view that coincides with $[Q', X']$ and is orthogonal to g'.

Lemma 5. *Referring to the notation in Theorem 2, the plane spanned by any characteristic k of $\mathcal{E}$ is a tangent plane τ_X to $\mathcal{C}$. The top view $[Q', M']$ of the tangent to q at the corresponding sphere's center Q passes through X' and is orthogonal to the top view of the generator $g \subset \tau_X$.*

Fig. 9 illustrates Lemma 5 in the skew case. The statement is trivial in the intersecting case since for each parabolic spine curve the lines $[Q', M']$ coincide with the top view of one torsal generator, while the cuspidal point of the other torsal generators serves as permanent contact point.

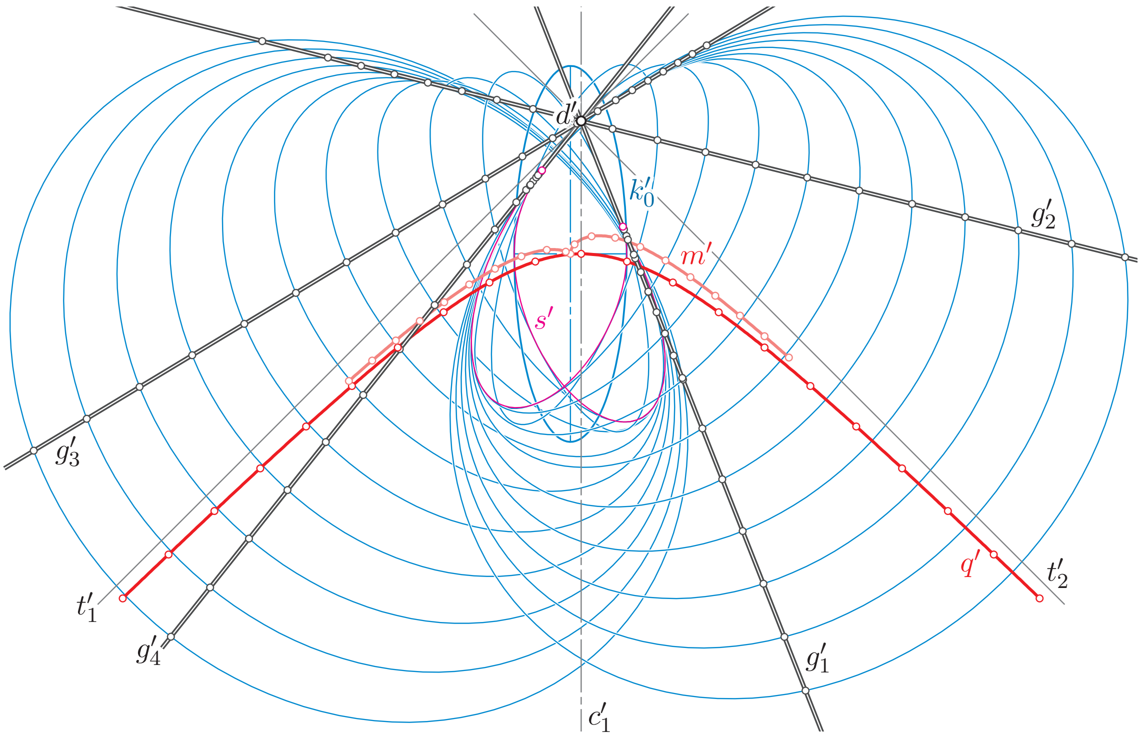

Figure 8: Top view of a sample of circles of one connected component of the canal surface $\mathcal{E}$ from Fig. 7. The hyperbola q' (red) is the top view of the spine curve and m' that of the curve of circle centers. The curve s' (magenta) is the top view of a cuspidal edge on $\mathcal{E}$.

4 Singularities

As mentioned before, each point of the spine curve q is the center of a sphere that contacts the four given lines g_i for $i = 1, \dots, 4$ at real points. However, the top view reveals that conversely not each point T of g_i needs to be a contact point with a real sphere of the one-parameter set. The line that connects T with the center $Q \in q$ of the contacting sphere must have a top view $[T', Q']$ which meets the equilateral hyperbola q' and is perpendicular to g_i'. This holds for all points $T' \in g_i'$ only if g_i' has no real intersection with q' (like g_2' and g_3' in Fig. 8).

Otherwise, there remains a segment on g_i' symmetric w.r.t. d' which is not subset of $\mathcal{E}$ (note g_1' and g_4' in Fig. 8). The terminating points are uniplanar points of $\mathcal{E}$, and the points T where $[T', P']$ meets the equilateral hyperbola q' twice are biplanar. Points of the inner segment are biplanar with complex conjugate tangent planes. We can summarize:

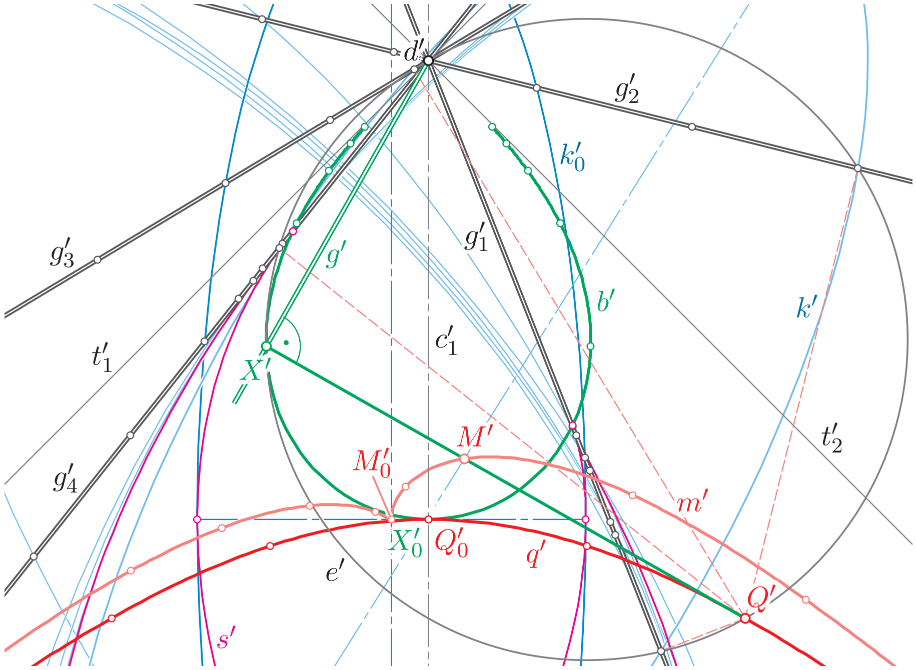

Figure 9: Zoom of Fig. 8. The planes of the characteristic circles k are tangent to the Plücker conoid $\mathcal{C}$ along the asymptotic curve $b \subset \mathcal{C}$ with the top view b' (green) in form of a lemniscate of Bernoulli. The curve s' (magenta) is the top view of the cuspidal edge of $\mathcal{E}$, while k_0' is the top view of the smallest characteristic.

Theorem 3. *Given four mutually skew concyclic lines $g_1, \dots, g_4$ on the Plücker conoid $\mathcal{C}$, let $\mathcal{E}$ be the envelope of the contacting spheres.*

The vertical planes through the torsal generators of $\mathcal{C}$ separate the space into two pairs of opposite sectors. A given line $g_i \subset \mathcal{C}$ belongs completely to the surface $\mathcal{E}$ and all points of g_i are regular for each component of $\mathcal{E}$ if and only if g_i lies in the sector which is disjoint to the spine curve q of $\mathcal{E}$.

Otherwise a segment of g_i symmetric w.r.t. the double line $d \subset \mathcal{C}$ lies in the exterior of $\mathcal{E}$, and the remaining halflines of g_i are curves of selfintersection for a component of $\mathcal{E}$.

The example displayed in Fig. 13 reveals that there exist cases where all four concyclic lines $g_1, \dots, g_4$ belong completely to both components. Fig. 7 shows a singularity-free part of an envelope $\mathcal{E}$ in the skew case.

4.1 The Curve of Characteristic's Centers

Theorem 4. *The center curve m of the circles k on the enveloping canal surface $\mathcal{E}$ is rational of degree ≤ 10.*

Proof. Let $P = (\xi, \eta, \zeta)$ be any point in space. First, we compute the corresponding pedal curve e on the Plücker conoid $\mathcal{C}$. The pedal points of the central generators c_1, c_2 w.r.t. P are the secondary vertices

$$C_1 = (\xi, 0, 0) \quad \text{and} \quad C_2 = (0, \eta, 0)$$

of the ellipse e. This yields for the semiaxes a, b of the ellipse e

$$4b^2 = \xi^2 + \eta^2 \quad \text{and} \quad a^2 = b^2 + c^2. \tag{9}$$

The principal vertices of e are the pedal points of the torsal generators t_1, t_2 w.r.t. P. Thus we obtain

$$T_1 = \frac{1}{2}(\xi+\eta,\, \xi+\eta,\, 2c) \quad \text{and} \quad T_2 = \frac{1}{2}(\xi-\eta, \eta-\xi, -2c).$$

The ellipse e has the center $\frac{1}{2}(\xi, \eta, 0)$. The plane ε of e is spanned by the direction vectors of the ellipse's axes, i.e., we obtain a normal vector of this plane ε as

$$\mathbf{n} = \begin{pmatrix} \xi \\ -\eta \\ 0 \end{pmatrix} \times \begin{pmatrix} \eta \\ \xi \\ 2c \end{pmatrix} = \begin{pmatrix} -2c\eta \\ -2c\xi \\ \xi^2+\eta^2 \end{pmatrix}.$$

Since ε passes through the vertex C_1 with position vector $\mathbf{c}_1$, it satisfies the equation

$$\varepsilon\colon\; -2c\eta x - 2c\xi y + (\xi^2+\eta^2)z = \mathbf{n}\cdot\mathbf{c}_1 = -2c\xi\eta. \tag{10}$$

If P with position vector $\mathbf{p}$ is a point of the spine curve of $\mathcal{E}$, then the center M of the characteristic circle k is the pedal point of ε w.r.t. P. This yields the position vector of M as

$$\mathbf{m} = \mathbf{p} + \frac{(\mathbf{c}_1-\mathbf{p})\cdot\mathbf{n}}{\mathbf{n}\cdot\mathbf{n}}\mathbf{n}, \tag{11}$$

hence

$$\begin{aligned}
\mathbf{m} &= \begin{pmatrix} \xi \\ \eta \\ \zeta \end{pmatrix} + \frac{2c\xi\eta - \zeta(\xi^2+\eta^2)}{(4c^2+\xi^2+\eta^2)(\xi^2+\eta^2)} \begin{pmatrix} -2c\,\eta \\ -2c\,\xi \\ \xi^2+\eta^2 \end{pmatrix} \\
&= \frac{1}{(4c^2+\xi^2+\eta^2)(\xi^2+\eta^2)} \begin{pmatrix} \xi(4c^2+\xi^2+\eta^2)(\xi^2+\eta^2) - 4c^2\xi\eta^2 + 2c\,\eta\zeta(\xi^2+\eta^2) \\ \eta(4c^2+\xi^2+\eta^2)(\xi^2+\eta^2) - 4c^2\xi^2\eta + 2c\,\xi\zeta(\xi^2+\eta^2) \\ \zeta(4c^2+\xi^2+\eta^2)(\xi^2+\eta^2) + 2c\,\xi\eta(\xi^2+\eta^2) - \zeta(\xi^2+\eta^2)^2 \end{pmatrix} \\
&= \frac{1}{(4c^2+\xi^2+\eta^2)(\xi^2+\eta^2)} \begin{pmatrix} 4c^2\xi^3 + 2c\eta\zeta(\xi^2+\eta^2) + \xi(\xi^2+\eta^2)^2 \\ 4c^2\eta^3 + 2c\xi\zeta(\xi^2+\eta^2) + \eta(\xi^2+\eta^2)^2 \\ 2c(2c\zeta+\xi\eta)(\xi^2+\eta^2) \end{pmatrix}.
\end{aligned}$$

From (9) follows

$$M = \frac{1}{4a^2b^2} \begin{pmatrix} c^2\xi^3 + 2b^2c\,\eta\zeta + 4b^4\xi \\ c^2\eta^3 + 2b^2c\,\xi\zeta + 4b^4\eta \\ 2b^2c(2c\,\zeta+\xi\eta) \end{pmatrix}. \tag{12}$$

If P runs along a rational curve, then m is rational, too. In the skew case, the spine curve q of $\mathcal{E}$ can be rationally parametrized as

$$\mathbf{q}(t) = \sqrt{\left|\frac{v}{u}\right|}\left(\frac{1+t^2}{1-t^2}, \frac{2t}{1-t^2}, w - \frac{t(1+t^2)}{c(1-t^2)^2}\sqrt{\left|\frac{v}{u}\right|}\right), \tag{13}$$

where by (8)

$$w := \frac{1}{2}\left[(z_1+z_2) + \frac{v(\cos 2\varphi_2 - \cos 2\varphi_1)}{u(z_1-z_2)}\right]. \tag{14}$$

The substitution of this parametrization in (12) confirms the claim. The top view m' of the characteristics' center curve m is depicted in the Figures 8 and 9. □

If any enveloping sphere on the canal surface $\mathcal{E}$ is smallest, then the tangent cone along the characteristic k is a cylinder and, consequently, the sphere's center Q coincides with the center M of the corresponding characteristic. From the representation in (11) follows the necessary condition

$$(\mathbf{c}_1 - \mathbf{p}) \cdot \mathbf{n} = 2c\xi\eta - \zeta(\xi^2 + \eta^2) = 0.$$

By (2), this is equivalent to $Q \in \mathcal{C}$.

For the points $Q \in q$, the semiaxes a, b of the pedal curve e by (9) are minimal if and only if Q' is a vertex of the equilateral hyperbola q'. Then a and b are stationary and the same holds for the radius of the coplanar characteristic k (note k_0' in Fig. 8).

Lemma 6. *Referring to the notation above, the smallest enveloping spheres of the envelope $\mathcal{E}$ have their centers at points where the spine curve q intersects the Plücker conoid $\mathcal{C}$. In the skew case the characteristic circle k and the coplanar pedal curve e are minimal if the corresponding center $Q \in q$ appears in the top view as vertex of the equilateral hyperbola q'.*

4.2 The Developable of Characteristics' Planes

Theorem 5. *Referring to the previous notation, the locus of the contact points X between the planes of the characteristics k of $\mathcal{E}$ and the Plücker conoid $\mathcal{C}$ is an asymptotic curve b of $\mathcal{C}$. Consequently, b is the line of regression of the developable $\mathcal{T}$ formed by the characteristics' planes. The curve b contacts at X the pedal curve $e \subset \tau_X$ of $\mathcal{C}$ w.r.t. the corresponding point $Q \in q$ and appears in the top view as a lemnniscate of Bernoulli b' (Fig. 9).*

Proof. The last statement is a direct consequence of Lemma 5 (note (Fig. 9): The locus b' of X' is the pedal curve of the equilateral hyperbola q' w.r.t. its center d'. Hence, b' is a lemnniscate of Bernoulli (note [2, p. 411]). It is well-known that these lemniscates are the top views of the asymptotic curves on $\mathcal{C}$ (see, e.g., [4, p. 216] or [5, p. 276]).

The planes τ_X corresponding to the points $Q \in q$ envelop the developable $\mathcal{T}$ which contacts the Plücker conoid $\mathcal{C}$ along the curve b. At each point $X \in b$, the generator of $\mathcal{T}$ and the tangent to b are conjugate w.r.t. $\mathcal{C}$. However, being self-conjugate the tangent to b coincides with the generator through X. This means that b is the line of regression (or cuspidal edge) of the developable $\mathcal{T}$.

Each tangent plane τ_X different from the torsal planes intersects $\mathcal{C}$ along an ellipse e and a line g (Fig. 2). The top view reveals that the asymptotic curve b must contact the ellipse e at X. □

For the sake of completeness we mention that for each given point $P = (\xi, \eta, \zeta)$ in space the plane τ_X of the pedal curve e contacts the Plücker conoid $\mathcal{C}$ at the point

$$X = \frac{1}{\xi^2 + \eta^2}\Big(\xi(\xi^2 - \eta^2), -\eta(\xi^2 - \eta^2), -2c\xi\eta\Big). \tag{15}$$

This follows from the curve of intersection between the tangent plane τ_X from (10) and $\mathcal{C}$ satisfying (2). The top view of this intersection obeys

$$(\eta x + \xi y)[(x^2 + y^2) - (\xi x + \eta y)] = 0.$$

By virtue of (7), $\xi^2 - \eta^2 = v/u$ is constant for the points Q on the spine curve q. Thus, the lemniscate of Bernoulli b' (Fig. 9) satisfies

$$u(x^2 + y^2)^2 - v(x^2 - y^2) = 0 \quad \text{or polar} \quad r^2 = \frac{v}{u}\cos 2\varphi.$$

The points of intersection between any characteristic k and the coplanar tangent to b are singular points of the envelope $\mathcal{E}$. Thus, we can obtain the edge of regression s of $\mathcal{E}$. The top view in the Figures 8 and 9 shows that the curve s' meets the lines g_1' and g_4' at their uniplanar points, and they seem to coincide with cusps of s'.

Corollary 2. *The intersection points between the characteristic circles k of the canal surface $\mathcal{E}$ and the respectively coplanar generators of the developable $\mathcal{T}$ form the cuspidal edge s of $\mathcal{E}$. Each canal surface through four mutually skew concyclic lines contains a cuspidal edge.*

Proof. As shown in Fig. 9, the principal vertex Q_0' of the hyperbola q' coincides with a vertex X_0' of Bernoulli's lemniscate b'. The tangent to b at X_0 is a slope line of the tangent plane τ_{X_0} and a diameter of the corresponding circle k_0. Therefore, the smallest characteristic k_0 (Lemma 6) contains two diametral singular points. Consequently, in the skew case the canal surface $\mathcal{E}$ can never be free of singularities (note Fig. 13). □

5 Symmetric Cases

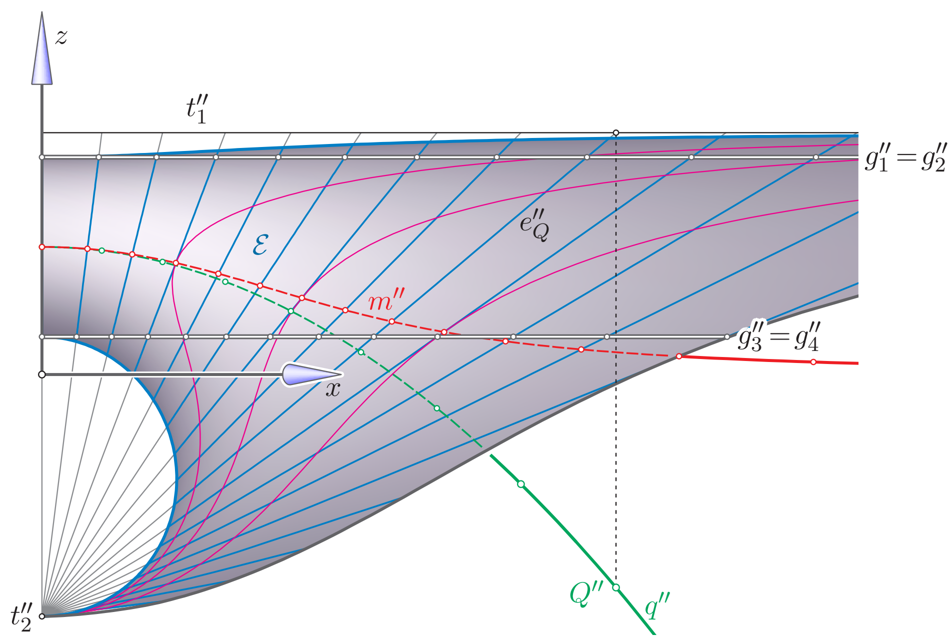

Figure 10: Orthogonal view of the right half of one component of the canal surface $\mathcal{E}$ in the intersecting case. The border of the depicted part of the surface is a contour line in a plane orthogonal to t_2. Other contour lines are shown in magenta.

We can distinguish between two symmetric cases where the centers M of the characteristics k are specified either on the principal axes (= slope lines) or on the secondary axes (= horizontal lines) of the respectively coplanar pedal curves, the ellipses $e \subset \mathcal{C}$. The cases of the first type are intersecting, the others are skew.

(a) In the intersecting case, the spine curve splits into two congruent parabolas (Theorem 2). One parabola opens to the positive z-axis, the other to the negative. We begin with the latter and confine us to one half of the parabola q in the vertical plane through the torsal line t_1. This plane is a plane of symmetry of the envelope $\mathcal{E}$. Figure 10 shows $\mathcal{E}$ after the orthogonal projection into this plane. We speak of a front view and indicate this by two primes. Note

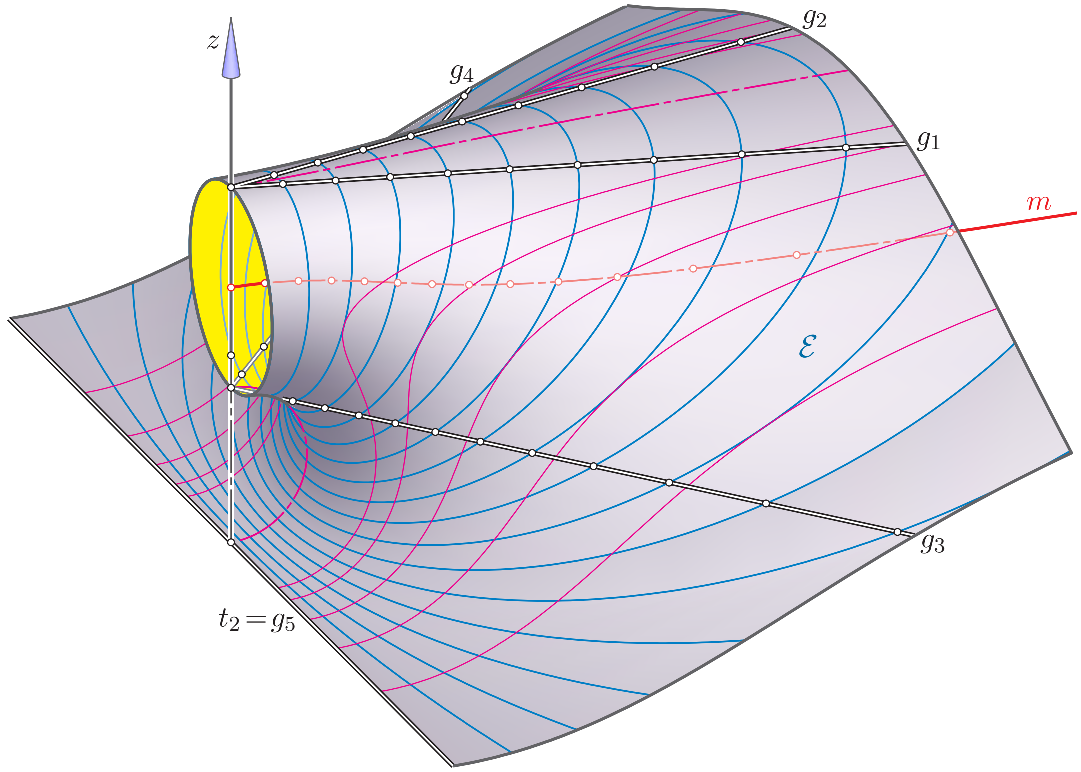

Figure 11: Axonometric view of one half of a component of the canal surface $\mathcal{E}$ in the intersecting case. The fifth line g_5 is the limit of a characteristic.

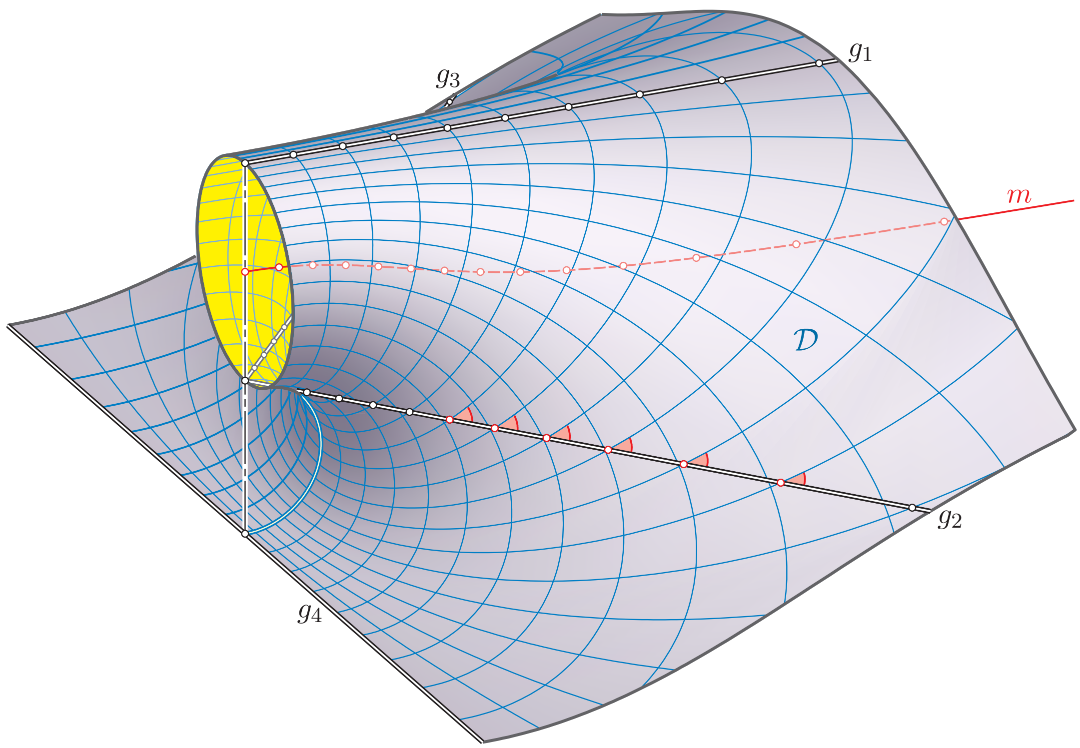

Figure 12: Axonometric view of one half of the parabolic Dupin cyclide as a limiting case of the intersecting envelopes (Fig. 10) with $g_1 = g_3$. With respect to its first generation as a canal surface, m (red) is the locus of characteristics' centers; the pedal points on the lines g_1, g_2, g_3 are marked, while g_4 is the limit of a characteristic.

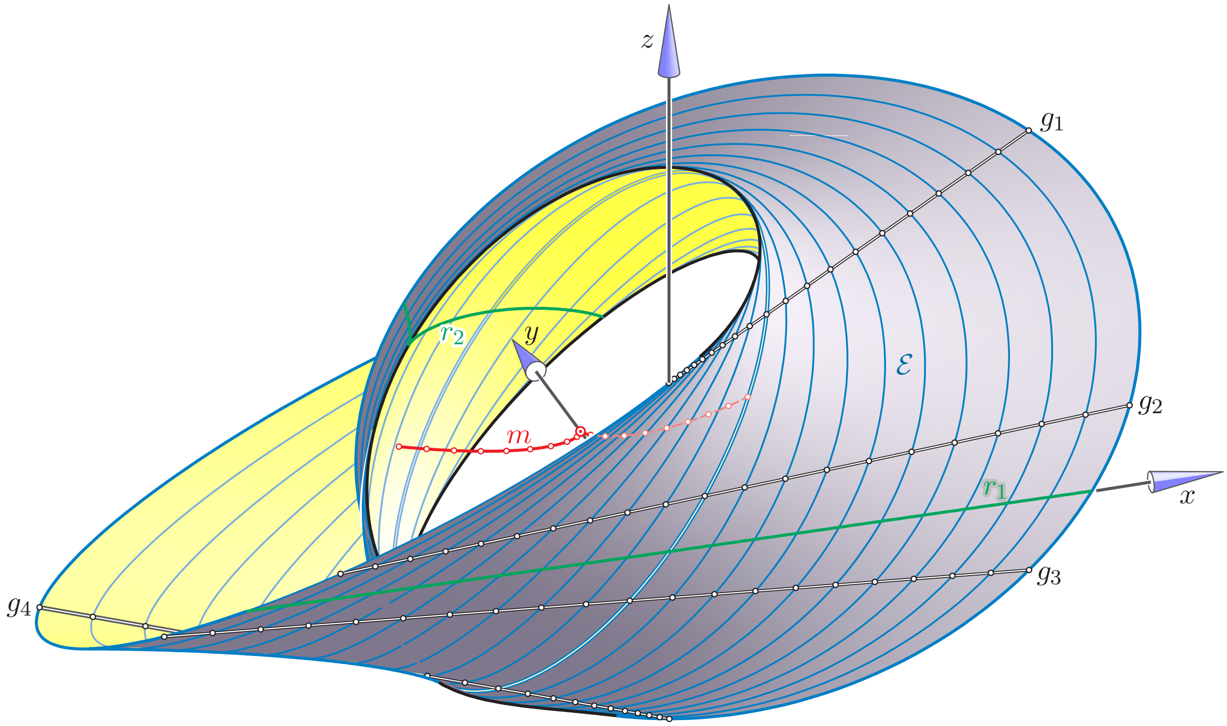

Figure 13: The canal surface $\mathcal{E}$ in the skew symmetric case. The black curves are visible cuspidal edges. The double line marks the smallest circle. The locus of the centers of the characteristics is denoted by m (red). The curves r_1 and r_2 (green) are the two components of the trace of $\mathcal{E}$ in the xy-plane.

that the images of the given lines g_1 and g_2 coincide as well as that of g_3 and g_4. By (15), the planes of the characteristic circles pass through the second torsal line t_2 of the Plücker conoid $\mathcal{C}$. When the sphere's center along the parabola q tends to infinity then the limit of the characteristic equals t_2. Hence, the envelope $\mathcal{E}$ contains a fifth line, however as the limit of a characteristic (note the axonometric view in Fig. 11).

We observe a similar behavior at parabolic Dupin ring cyclides where the spine curves of both generations as canal surfaces are two focal parabolas. Indeed, the envelope $\mathcal{E}$ in the intersecting case becomes a cyclide (Fig. 12) in the limiting case when g_1 and g_2 coincide with the torsal line $t_1 \subset \mathcal{C}$. Then, in Fig. 4 the circle k contacts the coplanar pedal curve e at a principal vertex, and the lines g_3 and g_4 are parabolic analogues of the Villarceau circles of ordinary Dupin ring cyclides [11, p. 154–155]. If the circle k is in 4-point contact with the pedal curve e at the principal vertex, then we obtain a parabolic Dupin needle cyclide [5, Fig. 10.18].

The second component of the envelope $\mathcal{E}$ looks similar. It's spine curve is a parabola open to the positive z-axis. This surface through $g_1, \dots, g_3$ turns upwards, and the torsal line t_1 is the characteristic of the limiting "sphere" with the center at infinity. The smallest circles of both components share the vertical diameter and the lowest and highest points, and they are located in orthogonal planes.

(b) In the symmetric skew case the centers M of the circles k are always located on the secondary axes of the pedal curves e. Consequently, the locus of the points M is a planar curve in the xy-plane.

As shown in Fig. 13, in this case the envelope has singularities in form of cuspidal edges like in all other skew cases. Apparently, at the specified example all points of the four lines are regular points of the displayed component of $\mathcal{E}$ (note Theorem 3). Since in this particular example two given lines g_2 and g_3 are close to the centerline c_1 of the Plücker conoid, the component r_1 of the traces of $\mathcal{C}$ in the xy-plane looks almost aligned. However, it would result in a contradiction with Corollary 1 if $\mathcal{E}$ contains five lines that contact all spheres.

References

[1] P. Appell: *Propriété caractéristique du cylindroïde.* Bulletin de la Société Mathématique de France **28**, 261–265, 1900.

[2] G. Glaeser, H. Stachel, and B. Odehnal: *The Universe of Conics. From the ancient Greeks to 21st century developments.* Springer Spektrum, Berlin, Heidelberg, 2016. ISBN 978-3-662-45449-7. doi: `10.1007/978-3-662-45450-3`.

[3] M. Husty and H. Sachs: *Abstandsprobleme zu windschiefen Geraden I.* Sitzungsberichte der österreichischen Akademie der Wissenschaften, Mathematisch-naturwissenschaftliche Klasse, Abteilung II **203**, 31–55, 1994.

[4] E. Müller and J. L. Krames: *Vorlesungen über Darstellende Geometrie. Band III: Konstruktive Behandlung der Regelflächen.* B.G. Teubner, Leipzig, Wien, 1931.

[5] B. Odehnal, H. Stachel, and G. Glaeser: *The Universe of Quadrics.* Springer Verlag, Berlin, Heidelberg, 2020. ISBN 978-3-662-61052-7, 978-3-662-61053-4. doi: `10.1007/978-3-662-61053-4`.

[6] G. Salmon and W. Fiedler: *Die Elemente der analytischen Geometrie des Raumes.* B.G. Teubner, Leipzig, 1863.

[7] M. Schilling: *Catalog mathematischer Modelle.* Martin Schilling, Leipzig, 7 ed., 1911.

[8] H. Stachel: *Unendlich viele Kugeln durch vier Tangenten.* Mathematica Pannonica **6**, 55–66, 1995.

[9] H. Stachel: *Plücker's Conoid Revisited.* Geodezia, Slovenský časopis Geometrie a Grafiky **19**(38), 21–34, 2022.

[10] T. Theobald: *New Algebraic Methods in Computational Geometry.* Habilitation thesis, Technische Universität München, 2003.

[11] W. Wunderlich: *Darstellende Geometrie I.* BI Mannheim, 1966.

[12] W. Wunderlich: *Darstellende Geometrie II.* BI Mannheim, 1967.

Received July 29, 2024; final form August 21, 2024.